# LANDSLIDE SUSCEPTIBILITY ASSESSMENT: SOIL MOISTURE MONITORING DATA PROCESSED BY AN AUTOMATIC PROCEDURE IN GIS FOR 3D DESCRIPTION OF THE SOIL SHEAR STRENGTH

S. Viaggio [1], A. Iacopino[1], R. Bovolenta[1], B. Federici[1*]

[1] Department of Civil, Chemical and Environmental Engineering (DICCA), University of Genoa,
via Montallegro 1, 16145 Genoa, Italy – stefania.viaggio@edu.unige.it,
(alessandro.iacopino, rossella.bovolenta, bianca.federici)@unige.it

**Commission IV, WG IV/4**

**KEY WORDS:** Soil moisture monitoring, soil shear strength, unsaturated conditions, landslides, GIS, water retention curve.

**ABSTRACT:**

Slope stability is strongly influenced by soil hydraulic conditions. Considering rain-triggered shallow landslides, the stability can be markedly influenced by the propagation of the saturation front inside the unsaturated zone. Soil shear strength varies in the vadose zone depending on the type of soil and the variations of soil moisture. Monitoring of the unsaturated zone can be done by measuring volumetric water content using low-cost instrumentation, such as capacitive sensors that are easy to manage and provide data in near-real time. For a proper soil moisture assessment a laboratory soil-specific calibration of the sensors is recommended. Knowing the soil water content, the suction parameter can be estimated by a Water Retention Curve (WRC), and consequently the soil shear strength in unsaturated conditions is evaluated. Several models are already proposed for shallow landslide susceptibility evaluation, also in FOSS GIS environment. However, these models do not usually consider the soil shear strength in unsaturated conditions, even if it is crucial, especially in the case of shallow landslides. A procedure that allows the estimate of the soil shear strength starting from soil moisture monitoring data (from sensor networks or satellite-derived map) is here presented. Moreover, preliminary results relative to a case study (i.e. the landslide of Ceriana-Mainardo in Italy) are shown. The proposed procedure could be integrated into existing models for landslide susceptibility assessment and also for the emergency management.

## 1. INTRODUCTION

Slope stability is strongly influenced by soil hydraulic conditions, affected by the meteoric events to which the site is subject. With particular reference to shallow landslides triggered by rainfalls, the stability conditions is influenced by the propagation of the saturation front inside the unsaturated zone. The soil shear strength varies in the vadose zone depending on the type of soil and the variations of soil moisture. Monitoring of the unsaturated zone can be done by measuring suction and/or water content.

The measurement of the soil volumetric water content can be performed through the use of low-cost capacitive sensors distributed over the study area. Such sensors provide data in near-real time and are relatively easy to install and replace. However, it is strongly recommended to perform a laboratory soil-specific calibration of the instrumentation, that should take into proper account the characteristics of the soil, where the sensors are installed (Campora et al., 2020). In fact, previous work (Bovolenta et al. 2020) has shown that the factory settings may lead to inaccurate estimates of the actual volumetric soil water content.

The knowledge of soil water content allows the estimate of the suction parameter, thanks to a Water Retention Curve (WRC), and consequently the definition of the soil shear strength in partly saturated conditions.

All the methodologies for landslide susceptibility assessment, based on the global Limit Equilibrium Method (LEM) or Finite Element Methods (FEM), need the soil shear strength description in order to evaluate the slope stability conditions. Both in the recent literature (Escobar-Wolf et al., 2021; Moresi et al., 2020) and in the GRASS GIS software (GRASS Development Team, 2022), models are already proposed for shallow landslide susceptibility evaluation in GIS, based mainly on LEM (e.g. *r.shalstab*). However, these models do not usually consider the unsaturated soil behaviour, but at most take into account the strength contribution provided by the vegetation root systems.

This paper proposes a procedure, developed as Python script in QGIS (QGIS Development Team, 2022), that, starting from soil moisture monitoring data, allows a spatially distributed estimate of the soil shear strength in the vadose zone, that is essential for the landslide susceptibility assessment, especially in the case of shallow landslides. In fact, in reference to 2D or 3D modeling, this procedure may be directly integrated in slope stability analyses in GIS environment, or its results may be adopted in LEM/FEM analyses. Its usefulness is significant in the analysis of shallow landslides, taking advantage of the soil moisture measurements to improve the evaluation of the stability conditions over time, by analysing the evolution of the saturation front according to the weather conditions. The monitoring of the water content in the soil can also be useful for the analysis of soil moisture conditions immediately after emergencies. In fact, the knowledge of the soil shear strength, calculated by the proposed procedure, is very important because landslide risk conditions may persist long after the officially issued alert has ceased. By the monitoring of the soil water content (provided that the sensors have not been damaged during the emergency) and by the soil shear strength evaluation, it would be possible to understand when people, subjected to evacuation, can return to their homes safely.

To support this procedure, some results obtained from the ana-

* Corresponding author

lysis of a case study (i.e. the landslide of Ceriana-Mainardo in Italy) are presented. Moreover, in order to allow the scientific community to evaluate the usefulness of the proposed procedure, both soil moisture data in Ceriana related to significant rainfall events and the implemented procedure will be openly shared, once the testing phase is completed.

## 2. AUTOMATIC PROCEDURE

The proposed procedure allows the evaluation of how shear strength varies in the ground as a result of changes in soil water content.
In the following the soil moisture monitoring data, the followed methodology, and the workflow of the proposed GIS procedure are described.

### 2.1 Soil moisture monitoring data

Capacitive sensors are considered the most suitable to monitor soil moisture and its changes induced by rainfalls: they are relatively inexpensive, easy to install and replace, and provide an almost immediate response to moisture variation. More specifically, capacitive sensors named WaterScout SM100 (Figure 1) were used.


Figure 1. WaterScout SM100.

The capabilities of the aforementioned devices have been analyzed by the University of Genoa in the context of the project AD-VITAM (Analysis of the Vulnerability of the Mediterranean Alpine Territories to natural risks), a cross-border cooperative project financed within the Interreg V-A France-Italie, ALCOTRA 2014-2020 (Bovolenta et al., 2020b).
Soil moisture sensors can be installed in the soil at different depths and at different locations in the analysed area, thus creating a monitoring network. The network may consist of a series of devices, called Sensor Pup (Figure 2), to which the capacitive sensors are plugged, and a receiver (Retriever), in turn connected to a Modem for remote data transmission (Figure 3).
Sensor Pups are distributed over the study area and each of them is usually connected to four soil moisture sensors. The sensors, placed at different depths, provide information on soil water content along a vertical measuring line. Communication between the Sensor Pups and the Retriever occurs via radio. Monitoring data are provided at time intervals ranging from 5 to 60 minutes as needed, and can be accessible and downloadable in .csv format through an internet portal (e.g. SpecConnect of Spectrum Tec.) and viewable through a mobile application (WatchDog Mobile). Each Sensor Pup is powered by 5 Watt solar panels. The same type of panel can power Modem and Retriever. However, it is also possible to connect them to the mains through a power adapter.
The installation of the described monitoring network requires some operational precautions to ensure communication between devices, their integrity over time and the reliability of the obtained measurements. First of all, it is necessary to position the Sensor Pups and the Retriever in such a way that the visibility between the devices ensures their proper communication. Then, it is recommended to fence the measurement nodes and prevent the generation of preferential infiltration paths when the

Figure 2. Sensor Pup positioned in Ceriana.

Figure 3. Retriever and Modem positioned in Ceriana.

sensors are inserted into the ground.
The calibration of soil moisture sensors is very important. Therefore, a soil-specific calibration has to be performed in laboratory, on soil samples taken directly from the study area where the sensors were installed, in order to define the correlation between the raw data and the actual volumetric water content (Bovolenta et al., 2020a).

### 2.2 Soil shear strength

In the vadose zone, the soil shear strength is strongly related to the soil features and to the variation of soil moisture, in terms of suction. For this reason, it is postulated the existence of a relationship between the unsaturated soil shear strength and the

soil-water characteristic curve (Vanapalli et al., 1996).
The use of Water Retention Curves (WRC) is probably the most widely employed method for defining the hydraulic characteristics of unsaturated porous media, such as soil. Indeed, the soil-water characteristic curve provides a conceptual and interpretative tool by which the behaviour of unsaturated soils can be understood (Vanapalli and Fredlund, 2000). However, as the definition of a site-specific WRC is not straightforward due to the requirement of specialized and expensive laboratory instrumentation, a variety of soil-water retention models have been proposed in literature.
In this work the described procedure for the definition of the WRC is based on the method proposed by Balzano et al. (2021), which employs the well-established pedotransfer function of Vereecken et al. (1989), built on a Van Genuchten (1980)-type function. The latter is based on a relationship directly linking volumetric water content and suction. It is worth underlining that the use of a pedotransfer function allows the use of empirical correlations between the water retention model and easily measurable physical soil properties. In particular, in the method here proposed, the Van Genuchten equation is related to intrinsic soil properties, (i.e. grain size distribution, dry density and carbon content). According to the Van Genuchten equation, the water retention curve of the reference soil can be written as follows:

$$\theta = \theta_r + (\theta_s - \theta_r)\frac{1}{1 + \left(\alpha \frac{s}{\gamma_w}\right)^n} \quad (1)$$

where $\theta$ = volumetric water content [-]
$s$ = suction [kPa]
$\theta_s$ = saturated volumetric water content [-]
$\theta_r$ = residual volumetric water content [-]
$\gamma_w$ = specific water weight = 10 kN/m$^3$
$\alpha$ = equation parameter [1/cm]
$n$ = equation parameter [-]

The introduced parameters are related to the intrinsic soil properties, grain size distribution, dry density and carbon content through the following relationships:

$$\theta_r = 0.015 + 0.005\%Clay + 0.014\%C \quad (2)$$

$$\theta_s = 0.81 - 0.283\rho_d + 0.001\%Clay \quad (3)$$

$$\alpha = exp(-2.486 + 0.025\%Sand - 0.351\%C + -2.617\rho_d - 0.023\%Clay) \quad (4)$$

$$n = exp(0.053 + 0.009\%Sand - 0.013\%Clay + -0.00015\%Sand^2) \quad (5)$$

where $\%Clay$ = clay fraction
$\%Sand$ = sand fraction
$\%C$ = carbon content
$\rho_d$ = soil dry density [g/cm$^3$]

The estimate of the dry density parameter is based on the assumption that the highest volumetric water content, $\theta_{max}$, recorded on field in occasion of significant rainfalls corresponds to the fully saturated soil state, thus coinciding with soil porosity. This assumption is expressed in terms of gravimetric water content, $w_{max}$:

$$\rho_d = \frac{\rho_w G_s}{1 + w_{max} G_s} \quad (6)$$

where $G_s$ = specific gravity of soil grains [-]
$\rho_w$ = water density = 1000 kg/m$^3$

The application of this model, through the estimate of the parameters involved, allows the definition of the specific WRC. Consequently, at any investigated vertical of the monitoring network, for each installation depth, knowing the volumetric water content values recorded by the capacitive sensors, the pertinent suction value is estimated as follows:

$$s = \frac{\gamma_w}{\alpha}\left(\frac{\theta_s - \theta}{\theta - \theta_r}\right)^{1/n} \quad (7)$$

where the meaning of the different parameters is explained above. According to the Eq. 8 proposed by Fredlund et al. (1978) and modified by Vanapalli et al. (1996), it is possible to estimate the value of unsaturated soil shear strength

$$\tau_f = c' + (\sigma - u_a)tan\phi' + (u_a - u_w)\left(\frac{S - S_r}{S_{max} - S_r}\right)tan\phi' \quad (8)$$

where $\tau_f$ = shear strength of an unsaturated soil [kPa]
$c'$ = effective cohesion [kPa]
$\phi'$ = effective angle of shearing resistance [°]
$(\sigma - u_a)$ = net normal stress on the plane of failure at failure [kPa]
$(u_a - u_w)$ = matrix suction, corresponding to the parameter s in the procedure described above [kPa]
$\left(\frac{S - S_r}{S_{max} - S_r}\right)$ = effective degree of saturation [-]

The procedure described in the following is devoted to calculate the third addendum of Eq. 8, which is strictly related to unsaturated soil conditions.

### 2.3 GIS procedure flow

The proposed automatic procedure in GIS environment allows to describe the evolution of the saturation front inside the vadose zone according to soil moisture measurements given the weather conditions. This procedure is based on a Python script implemented in QGIS.
Taking into account the unsaturated soil behaviour, the developed methodology allows the soil shear strength evaluation, which is fundamental for the stability assessment, with particular reference to shallow landslides.
The estimate of the unsaturated soil shear strength first requires the definition of a site-specific Soil Water Retention Curve. The procedure adopts the method proposed by Balzano et al. (2021), detailed in the Section 2.2.
The implemented method requires as input data the intrinsic soil properties and the maximum water content value ($\theta_{max}$), corresponding to a fully saturated soil condition, registered on site by the monitoring network over all the period of measurements. The user must therefore provide as input the percentages of sand, clay, carbon content and $\theta_{max}$. The implementation of the formulas allows to estimate the parameters involved ($\alpha$ , $n$, $\theta_s$, $\theta_r$, $w_{max}$ and $\rho_d$) and consequently the definition of the site specific Soil-WRC.
Obviously, the Volumetric Water Content (VWC) values are requested in input, in order to calculate the pertinent soil shear strength values.
VWC data can be provided as punctual data or in a raster format, by using maps obtained from point data interpolation or remote sensing product processing. In case of data provided by a monitoring network as punctual data, they can be stored in a geodatabase, and the user can choose the time scale to work with. Once the rainfall period to be analysed is identified, the raw data at the different installation depths are extracted

for each node composing the monitoring network. Otherwise, the user can provide a .csv or .txt input format containing data downloaded by the network.
Input VWC data can be either raw or already calibrated. In the case of VWC data requiring calibration, the procedure allows the user to enter the calibration parameters, according to a linear relationship.
By entering the relevant VWC values in the Soil-WRC curve, the automatic procedure performs the suction calculation at each node, by applying the Eq. 7 in Section 2.2, for each measurement depth, related to each day.
Spatialising this information at different depths, by applying the Delaunay triangulation interpolation between the nodes, the final products are surfaces of unsaturated shear strength over the investigated area.
If the VWC input data are already provided in raster format, i.e. already distributed over the study area, the previous formulas are applied to each cell of the raster, and spatial interpolation is not necessary.

## 3. APPLICATION TO THE CERIANA CASE STUDY

In the framework of the Interreg Alcotra AD-VITAM project, in December 2019, a soil moisture monitoring network of the type described in Section 2.1 was installed at Ceriana-Mainardo (IM), located in the west part of the Liguria Region (Figure 4). This site has been chosen for its well-known landslide susceptibility triggered by rainfall.
The monitoring network, currently operational, consists of five measurement nodes (named C1, C2, C3, C4, C5) distributed over the study area, each bearing four soil moisture sensors positioned at different depths (-10, -35, -55 and -85 cm) along a vertical, as detailed in Section 2.1 (Bovolenta et al., 2020a).
In the here proposed case study, the analysed meteorological event corresponds to the better-known storm named Alex (for brevity indicated as Alex Storm in the following), which occurred between the 01/10/2020 and 02/10/2020, when approximately 250 mm of rain was recorded by the rain gauge in 48 hours. The authors decided to consider a few days before, when a significant rainfall of 52 mm occurred, (so starting from 22/09/2020), in order to have a better characterisation of the unsaturated shear strength behaviour in the vadose zone as well as to include a rain event that may occur with a higher occurrence.

### 3.1 Input data

According to the workflow explained in Section 2.3, the automatic procedure for the application of the site-specific unsaturated Soil VWC-shear strength relationship requires the definition of intrinsic soil properties as input data. These quantities were determined by performing a geotechnical characterisation and a VWC laboratory calibration on the Ceriana-Mainardo soil.
The grain size distribution by sieving and sedimentation for a soil sample at node C5 was conducted conforming to the guidelines proposed by BS EN ISO 17892-4:2016. Furthermore, with reference to a soil sample at the C3 node, the carbon content was calculated as 58% of the soil organic matter (Pribyl, 2010), determined in compliance with the standard ASTM D2974-20 (2020). The soil values adopted as input in the automatic procedure are shown in Table 1.
For the case study, $G_s$ is equal to 2.6. and it was determined through of a picnometer test according to BS EN ISO 17892-3:2015.

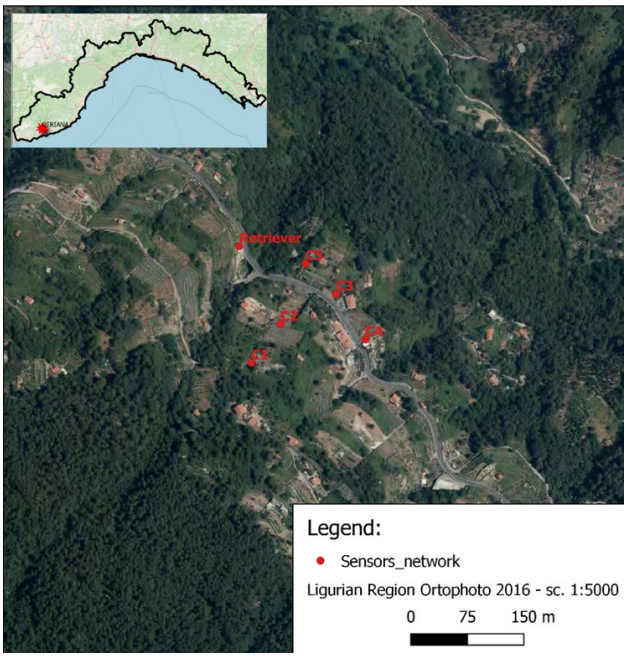


Figure 4. Overview of Ceriana-Mainardo and the soil moisture monitoring network.

| $\%Sand$ | $\%Clay$ | $\%C$ |
|---|---|---|
| (%) | (%) | (%) |
| 47.9 | 29.0 | 1.304 |

Table 1. Intrinsic soil properties

Concerning the VWC value, the monitoring sensor network installed on site provide raw data (see Section 2.1), for which a soil-specific VWC calibration is needed. For this reason the laboratory calibration was performed on a soil sample referring to node C5. In particular, the sample has been de-structured and divided into several specimens, which were then moistened with different amounts of water to simulate water content variations. This methodology has provided the VWC soil-specific calibration equation for the Ceriana-Mainardo site by a linear regression of the laboratory data (Figure 5).

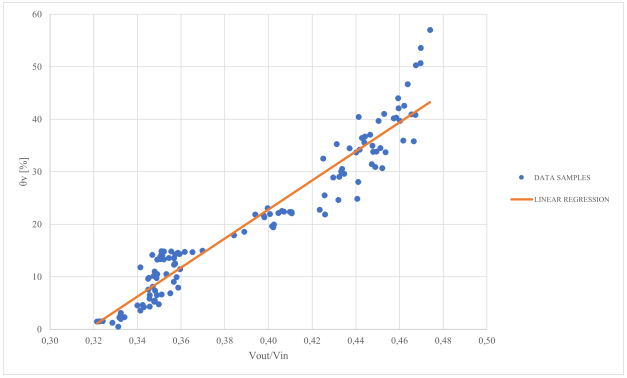


Figure 5. Laboratory sensors calibration equation.

The equation is defined as follows:

$$\theta_v = a\left(\frac{V_{OUT}}{V_{IN}}\right) + b \tag{9}$$

where $\left(\frac{V_{OUT}}{V_{IN}}\right)$ = normalised ratio between raw data $V_{OUT}$ measured by the field sensors and the input voltage $V_{IN}$ of Sensor Pup

$a, b$ = constants, respectively equal to 276.5 and -87.8, provided by the linear regression, as shown in the Figure 5.

This linear correlation allows the transition from the raw data, duly normalised to the Sensor Pup input voltage, to the estimated VWC value (in the follows defined as $\theta_v$) at any given depth. By applying this equation on the maximum data measured by the network over the period May 2020-March 2022, the calibrated $\theta_{max}$ value results equal to 0.478. With reference to the calibrated $\theta_{max}$ adopted in the procedure, the calculated gravimetric water content value and the pertinent dry density value are equal to 0.352 and 1.357 $g/cm^3$ respectively.
The authors decided to work on a daily time scale. For this reason, with reference to the above mentioned period, the raw data for each node, corresponding to the 24 hours of recording, were extracted from the geodatabase in .csv format and opened in the Python script. Then the Eq. 9, implemented in the procedure, allowed to estimate the calibrated $\theta_v$ values.

### 3.2 Results

Once all the input data were set, the implemented procedure performed the calculation of the WRC for the Ceriana-Mainardo soil. In Figure 6 the suction (in kPa) is reported in abscissa on a logarithmic scale, in accordance with the literature representation, and the $\theta_v$ (dimensionless) is indicated on the ordinate. The blue line represents the WRC obtained for the Ceriana-Mainardo soil type, the orange line represents the residual volumetric water content, $\theta_r$ , while the black dot is $\theta_s$, corresponding to a fully saturated soil condition.

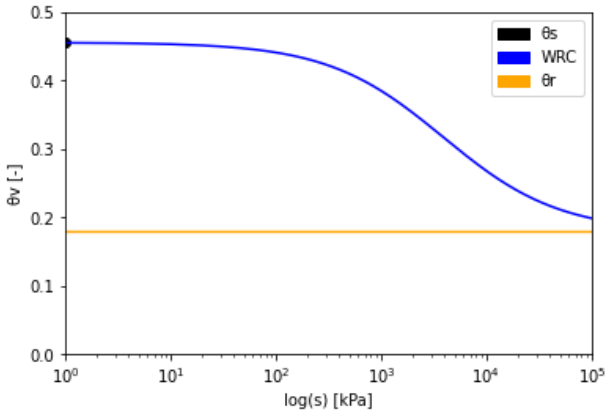


Figure 6. Soil-WRC.

With reference to each measurement depth, the suction value was calculated by applying Eq. 7 during the rainfall period.
Finally, the shear strength of the unsaturated soil was also evaluated according to Eq. 8.
The last step performed by the procedure is the interpolation between the soil shear strength values at each node, applying the Delaunay triangulation technique, in order to spatialise the information over the area of interest.
The outputs of the automatic procedure are the shear strength surfaces induced by partial saturation, as specified in section 2.2, at the four measurement depths, related to each day of the analysed period.
Three maps, related to the depth equal to -35 cm, are showed in Figures 7, 8 and 9, in order to represent the unsaturated shear strength variation according to the rainfall intensity. The colour scale varies from blue to red according to a decrease of unsaturated soil shear strength.

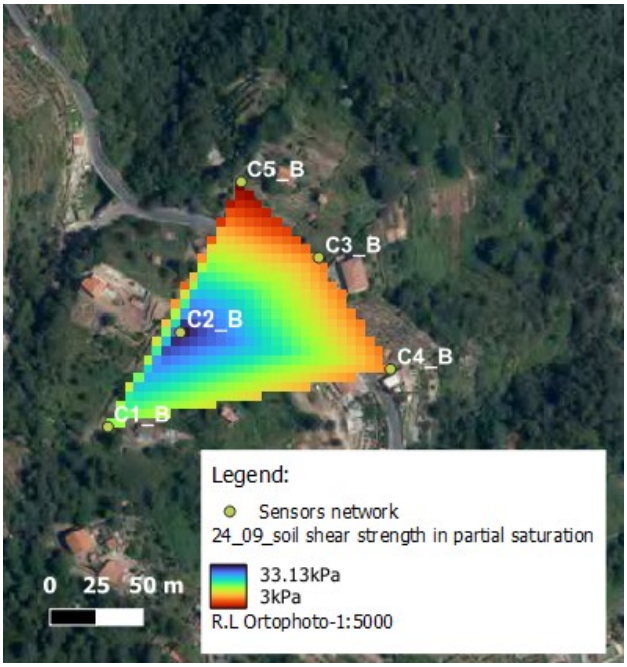


Figure 7. The shear strength surface induced by partial saturation referring to 24/09/2020, after the first significant rainfall occurred on 22/09/2020.

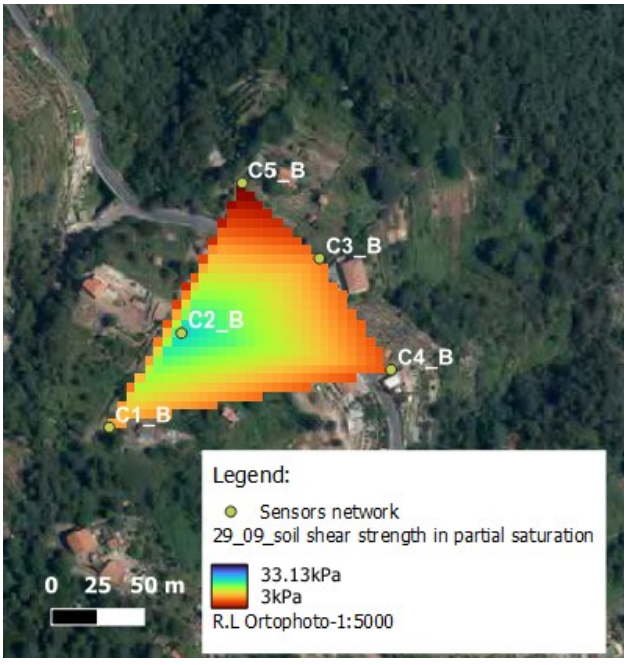


Figure 8. The shear strength surface induced by partial saturation referring to 29/09/2020, a dry day between the two analysed rainfalls.

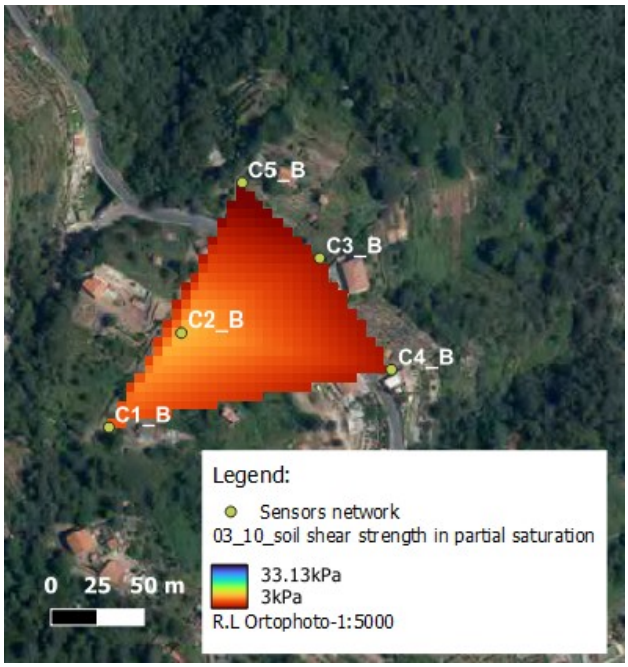


Figure 9. The shear strength surface induced by partial saturation referring to 03/10/2020, after the Alex Storm.

Figure 7 represents the unsaturated soil shear strength conditions on 24/09/2020, after the first medium-intensity rainfall day, occurred on 22/09/2020. High unsaturated soil shear strength values characterised the upper part of the investigated area, while lower values characterised the deeper one. After the rainfall of 22/09/2020, the unsaturated soil shear strength decreases as a consequence of an increasing in the soil saturation, denoting a higher volumetric water content in the soil, as showed in Figure 7.

Figure 8, relating to 29/09/2020, shows a further decrease in the shear strength of the soil, evidenced by a fading of the colour scale, due to the rainfall that occurred a few days before. However, the map still shows higher unsaturated soil shear strength values in the middle of the study area.

Completely different scenario is shown in Figure 9 concerning the day following the Alex Storm (03/10/2020), where a severe decreasing of soil shear strength in unsaturated conditions is highlighted. Note that red color indicates very low value of shear strength induced by partial saturation.

Figure 10 shows the shear strength induced by partial saturation (in grey) with reference to each day of the analysed period, where rainfall is represented by the blue histogram, also compared with the monitored VWC values (in orange). The graph was obtained by querying the raster outputs of the automatic procedure at the -35 cm depth in the node C3. Note that, for a better comprehension of the parameters showed in the graph, the shear strength value are multiplied by 10.

With regard to the VWC trend, a good response to rainfall is evident, with high values during moderate (22/09/2020) or intense (01-02/10/2020) rainfalls. Conversely, the shear strength shows a significant decrease when rainfall occurs. This trend is linked to the variation in soil moisture content, as shown in Figure 10.

The results of this application show the magnitude of these variations, which can have an important effect on slope stability.

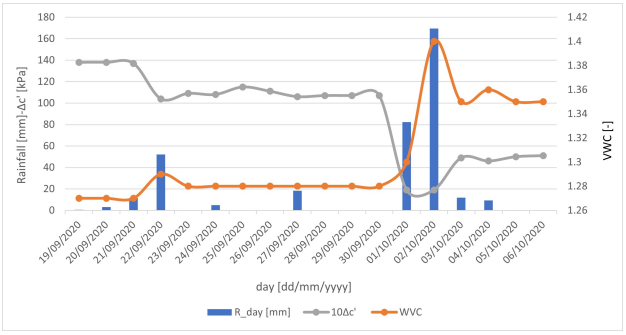


Figure 10. Shear strength induced by partial saturation (grey line) and volumetric water content (orange line) over the days of the analysed period (22/09/2020-06/10/2020). The shear strength value are multiplied by 10.

## 4. CONCLUSION

In the present paper, an automatic procedure, implemented in QGIS via a Python script, has been formulated in order to provide a 3D description of the soil shear strength in the vadose zone.

Soil moisture monitoring data, coming from a sensor network, feed a properly structured table in a geodatabase, or they can be provided as a raster map, obtained from point data interpolation or remote sensing product processing. If data are not already calibrated, the equation of the soil-specific sensor calibration, defined in laboratory, is applied in order to pass automatically from the raw sensor data to the soil water contents.

Then the equation of the WRC is applied to evaluate the suction, and the soil shear strength induced by partial saturation can be estimated for each depth at which a soil moisture sensor is installed.

If the input data come from a monitoring network, the output values must be spatialized over the entire area of interest, through appropriate techniques of interpolation.

The application of the implemented procedure to the Ceriana-Manairdo landslide, relating to a significant rainfall period, occurred between the end of September and the beginning of October 2020, was presented. The description of the soil moisture monitoring network installed on site, the specific soil retention curve, and the resulting shear strength maps induced by partial saturation were shown. The Delaunay triangulation interpolation algorithm between the nodes of the monitoring network proved to be a good technique for the production of the strength surfaces.

The knowledge of unsaturated soil behaviour is essential for the landslide susceptibility assessment, especially in the case of shallow landslides. The described procedure could be usefully integrated into several landslide models, taking advantage of the soil moisture measurements to improve the evaluation of the stability conditions over time, by analysing the evolution of the saturation front according to the weather conditions. For example, the produced strength maps can be set as input data in the GRASS GIS command *r.shalstab*[1] for shallow landslides susceptibility assessment based on LEM method. Actually, this module does not consider the unsaturated soil behaviour, but only takes into account the strength contribution provided by the vegetation root systems. The integration of the present procedure might improve it.

The authors will integrate it into a system called LAMP (LAndslide Monitoring and Predicting) (Bovolenta et al., 2016),

[1] https://grass.osgeo.org/grass78/manuals/addons/r.shalstab.html

based on the implementation in GRASS GIS of an Integrated Hydrological-Geotechnical (IHG) 3D model (Passalacqua et al., 2012; Bovolenta et al., 2017) for the landslide susceptibility assessment triggered by measured or forecasted rainfalls. The integration of this procedure in LAMP will allow to obtain a simple but effective modeling for the assessment of susceptibility to shallow landslides.
Moreover, several software for landslide susceptibility assessment can use the output maps of the present procedure.
This contribution can usefully improve existing tools for technicians involved in risk management to assess susceptibility to shallow landslides.

## ACKNOWLEDGEMENTS

The authors wish to thank Estelle Stefanini, student at the Ecole Nationale des Sciences Géographiques (ENSG), for the implementation of the Python script during her internship.

## REFERENCES

Balzano, B., Bruno, A. W., Denzer, H., Molan, D., Tarantino, A., Gallipoli, D., 2021. REAL-TIME quality check of measurements of soil water status in the vadose zone. *Physics and Chemistry of the Earth, Parts A/B/C*, 121, 102918. DOI: https://doi.org/10.1016/j.pce.2020.102918.

Bovolenta, R., Federici, B., Berardi, R., Passalacqua, R., Marzocchi, R., Sguerso, D., 2017. Geomatics in support of geotechnics in landslide forecasting, analysis and slope stabilization. *In GEAM, Geoingegneria Ambientale e Mineraria - ISSN: 1121-9041*, 151(2), 57–62.

Bovolenta, R., Iacopino, A., Passalacqua, R., Federici, B., 2020a. Field measurements of soil water content at shallow depths for landslide monitoring. *In Geosciences (Switzerland) - ISSN: 2076-3263*, 10(10), 409. DOI: 10.3390/geosciences10100409.

Bovolenta, R., Passalacqua, R., Federici, B., Sguerso, D., 2016. LAMP-LAndslide Monitoring and Predicting for the analysis of landslide susceptibility triggered by rainfall events. 2, 517–522. DOI: 10.1201/9781315375007-45.

Bovolenta, R., Passalacqua, R., Federici, B., Sguerso, D., 2020b. Monitoring of Rain-Induced Landslides for the Territory Protection: The AD-VITAM Project. In Lecture Notes in Civil Engineering - ISSN: 2366-2557. 40, 138–147. DOI: 10.1007/978-3-030-21359-6_15.

Campora, M., Palla, A., Gnecco, I., Bovolenta, R., Passalacqua, R., 2020. The laboratory calibration of a soil moisture capacitance probe in sandy soils. *Soil and Water Research - ISSN: 1801-5395*, 15(2), 75–84. DOI: 10.17221/227/2018-SWR.

Escobar-Wolf, R., Sanders, J., Vishnu, C., Oommen, T., Sajinkumar, K., 2021. A GIS tool for infinite slope stability analysis (GIS-TISSA). *Geoscience Frontiers*, 12(2), 756–768.

Fredlund, D., Morgenstern, N. R., Widger, R., 1978. The shear strength of unsaturated soils. *Canadian geotechnical journal*, 15(3), 313–321. DOI: https://doi.org/10.1139/t78-029.

GRASS Development Team, 2022. Geographic Resources Analysis Support System (GRASS) Software. Open Source Geospatial Foundation. https://grass.osgeo.org, last accessed on 08 June 2022.

Moresi, F., Maesano, M., Collalti, A., Sidle, R., Matteucci, G., Scarascia Mugnozza, G., 2020. Mapping landslide prediction through a GIS-based model: A case study in a catchment in southern Italy. *Geosciences*, 10(8), 309.

Passalacqua, R., Bovolenta, R., Spallarossa, D., De Ferrari, R., 2012. Geophysical site characterization for a large landslide 3-D modeling. In Proceedings of the Fourth International Conference on Geotechnical and Geophysical Site Characterization ISC'4 - ISBN:9780415621366. 2, 1765–1771.

Pribyl, D. W., 2010. A critical review of the conventional SOC to SOM conversion factor. *Geoderma*, 156(3-4), 75–83. DOI: https://doi.org/10.1016/j.geoderma.2010.02.003.

QGIS Development Team, 2022. QGIS Geographic Information System. https://www.qgis.org, last accessed on 08 June 2022.

Van Genuchten, M. T., 1980. A closed-form equation for predicting the hydraulic conductivity of unsaturated soils. *Soil science society of America journal*, 44(5), 892–898. DOI: https://doi.org/10.2136/sssaj1980.03615995004400050002x.

Vanapalli, S., Fredlund, D., 2000. Comparison of different procedures to predict unsaturated soil shear strength. 195–209. DOI:https://doi.org/10.1061/40510(287)13.

Vanapalli, S., Fredlund, D., Pufahl, D., Clifton, A., 1996. Model for the prediction of shear strength with respect to soil suction. *Canadian geotechnical journal*, 33(3), 379–392. DOI:https://doi.org/10.1139/t96-060.

Vereecken, H., Maes, J., Feyen, J., Darius, P., 1989. Estimating the soil moisture retention characteristic from texture, bulk density, and carbon content. *Soil science*, 148(6), 389–403. DOI:10.1097/00010694-198912000-00001.